

# Pharos: Enable Physical Analytics through Visible Light based Indoor Localization

Pan Hu<sup>1</sup>, Liqun Li<sup>2</sup>, Chunyi Peng<sup>3</sup>, Guobin Shen<sup>2</sup>, Feng Zhao<sup>2</sup>

<sup>1</sup>UMass Amherst; <sup>2</sup>Microsoft Research, Beijing, China; <sup>3</sup>Ohio State University

<sup>1</sup>panhu@cs.umass.edu; <sup>2</sup>{liqun, jackysh, zhao}@microsoft.com; <sup>3</sup>chunyi@cse.ohio-state.edu

## ABSTRACT

Indoor physical analytics calls for high-accuracy localization that existing indoor (e.g., WiFi-based) localization systems may not offer. By exploiting the ever increasingly wider adoption of LED lighting, in this paper, we study the problem of using visible LED lights for accurate localization. We identify the key challenges and tackle them through the design of Pharos. In particular, we establish and experimentally verify an optical channel model suitable for localization. We adopt BFSK and channel hopping to achieve reliable location beaconing from multiple, uncoordinated light sources over shared light medium. Preliminary evaluation shows that Pharos achieves the 90th percentile localization accuracy of 0.4m and 0.7m for two typical indoor environments. We believe visible light based localization holds the potential to significantly improve the position accuracy, despite few potential issues to be conquered in real deployment.

## Categories and Subject Descriptors

C.2.1 [Network Architecture and Design]: Wireless communication; C.3.3 [Special-Purpose and Application-based Systems]: Real-time and embedded systems

## General Terms

Design, Experimentation, Performance

## Keywords

Visible light, Optical channel model, LED, Mobile, Indoor localization, Physical analytics

## 1. INTRODUCTION

Physical analytics is a rising technique to understand and better design the physical space [2, 3]. By monitoring and

analyzing user actions and environment events, such analytics would be valuable in a variety of contexts, for example, physical retailers track shoppers and gain analytics of their interests for optimal store layouts and customized coupons offerings [16, 13, 19], or a tradeshow or a museum fine-tunes its layout based on the physical browsing patterns of users.

To provide in-depth physical analytics and to precisely navigate the user, it calls for high accuracy indoor localization. Existing solutions rely mostly on WiFi-based positioning technologies, which usually deliver an accuracy of up to few meters [7, 22, 4]. Such accuracy is amenable for coarse-grained physical analytics such as how long customers stay at different areas of the store. However, it cannot provide more detailed information such as which particular shelf or particular brand(s) at different heights in a shelf a user has paused at. Such fine-grained analytics would reveal more valuable information to not only the shop owners but also the manufacturers of specific brands. On the customers side, it is also very desirable if a customer can be directly navigated to the small proximity of the actual product (s)he is looking for.

To this end, we propose *Pharos*, a novel sub-meter localization system exploiting the Light-emitting Diode (LED) lighting infrastructure. We choose LED lighting for its ever increasingly wider adoption and dual-paradigm feature (i.e., communication as well as illumination). LED is a new lighting technique and enjoy several advantages as compared with compact fluorescent light (CFL) bulbs such as higher energy efficiency (2x), much longer lifetime (6x); constant lighting efficiency throughout the whole lifespan [1], mercury free and thus more environment friendliness, to name a few. More importantly, LED also possesses another feature – instantaneous on and off. For instance, we measured the rising and falling edges of an ordinary commodity LED bulb are only about  $4\mu s$ . This feature allows LEDs to be dimmed via Pulse Width Modulation (PWM) and enables visible light communication (VLC), which has been studied for years [12, 10] and is recently standardized in IEEE 802.15.7 [18].

The major goal of Pharos is *to provide high positioning accuracy in a low(zero)-cost and easy-to-use fashion*. It has three-fold implications. First, it reuses the existing lighting system for the localization purpose and can be gradually

Permission to make digital or hard copies of all or part of this work for personal or classroom use is granted without fee provided that copies are not made or distributed for profit or commercial advantage and that copies bear this notice and the full citation on the first page. To copy otherwise, to republish, to post on servers or to redistribute to lists, requires prior specific permission and/or a fee.

*Hotnets '13*, November 21–22, 2013, College Park, MD, USA.

Copyright 2013 ACM 978-1-4503-2596-7 ...\$10.00.

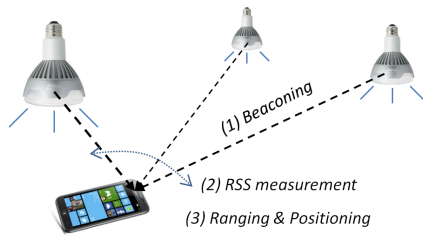


Figure 1: Conceptual overview of Pharos.

enabled. Second, Pharos does not depend on any centralized localization service (e.g., a localization database in the WiFi-based solutions). Ideally, the system should be capable of “plug-and-play”. It facilitates receiver-side localization so that a device (e.g., a modern smartphone) can infer its position at a minimum interaction (passive listening, here) with the lighting infrastructure. Last but not least, Pharos is able to yield high accuracy (sub-meter) localization. In fact, it is promising to achieve unprecedented localization accuracy by leveraging the lighting system rather than other infrastructure-based systems (e.g., WiFi-based) for two reasons. (1) The deployment of illumination lights is much (over one order of magnitude) denser than that of an WiFi access point (AP). For example, in our office floor, there are about 21 APs that covers the whole floor whereas over 300 light sources are deployed to cover the same space. (2) Visible light has much short wavelengths than WiFi radio, which implies much less severe multipath effects. Moreover, light sources, unlike WiFi radio signals, are always visible. It exposes a unique opportunity to involve the user into the positioning loop in some challenging scenarios.

The mere challenge is how to leverage these favorable facts. We design Pharos to exploit optical channels for localization purpose. It works as follows (Figure 1): each bulb, in addition to its major lighting role, also serves as a location landmark. It broadcasts, via the light carrier, beacons carrying information, i.e., the position of the bulb and its duty cycle, to facilitate receiver side localization. A receiver (e.g., a mobile phone) employs a light sensor to retrieve the beacon information, and measures RSSes from multiple bulbs and computes the distances to each bulb through the proposed channel model. Finally, it estimates its location based on the received beacon information and distance measurements from all light sources. In Pharos, there are three key enabling techniques.

- First, we perform accurate distance measurement between a light source and a receiver. We establish and experimentally verify an optical channel model for localization purpose. That is, we relate the distance to the received signal strength (RSS), explicitly considering the possibility that a light lamp might be dimmed in actual use (§2).
- Second, we enable reliable information transmission over *shared* light medium. We exploit the visible light for communication capability of LED to *directly* broadcast via the visible light carrier the location beacons to a receiver

device. In order to grant multiple, uncoordinated light communications, we adopt binary frequency shift keying (BFSK) modulation scheme, and mitigate possible collisions through channelization and hopping (§3).

- Third, we obtain precise localization through multilateration techniques. The location beacon contains the position of the LED and its duty cycle, to facilitate receiver side localization. The collected beacon(s), together with measured RSSes, are used to infer the receiver’s position. As a result, the provider can simply configure the LED and plug it in, the localization service is instantly enabled (§4).

We have implemented the Pharos prototype, for which we deploy five small LED bulbs and a mobile phone that connects with a light sensor board through its audio jack. We perform preliminary evaluation of Pharos in typical office environments, including a conference room and a cubicle area. They represent different environmental complexity and usual light deployment. The experimental results confirm that using visible light yields high localization accuracy: the 90th percentile accuracy is 0.4m for the conference room, 0.7m for the cubicle area (around 0.3m for the average case). Though some potential issues need to be addressed, we believe the system can be further optimized to achieve an accuracy level suffice for physical analytics.

## 2. ESTABLISHING THE CHANNEL MODEL

Localization is typically realized through multilateration or multiangulation approaches. Since a light sensor is usually omni-directional, multiangulation is not applicable. We adopt multilateration approach. The prerequisite condition is to establish a model that can precisely relate the received light strength to the distance to the light source.

### 2.1 General Optical Channel Model

For an optical wireless link, the received energy over one channel can be calculated as

$$P_r = P_t \cdot H(d) \cdot G_r \quad (1)$$

where  $P_t$  is the transmission power (over the channel) of the light source,  $H(d)$  is the the channel gain that is related to the actual sender-receiver distance  $d$ , and  $G_r$  is the receiver gain which can be calibrated once for good. The radiant intensity of a LED chip is usually assumed to follow a Lambertian radiation pattern [5]. Then, the channel gain can be generally modeled by Eq. (2)

$$H(d) = A \cdot g(\phi) \cdot \left[ \frac{m+1}{2\pi} \right] \cdot \cos^m \phi \cdot \frac{\cos \theta}{d^2} \quad (2)$$

where  $A$  is the area of the sensor detector,  $\phi$  and  $\theta$  are the irradiation angle and the incidence angle, as depicted in Figure 2.  $g(\phi)$  is called the optical concentrator which is a constant if the incidence angle falls in the field of view of the sensor detector [12].  $m$  is called the Lambertian order.

However, this generic optical link model cannot be directly applied for the localization purpose. We need to determine the parameters of the model (e.g., the order  $m$ ) and also

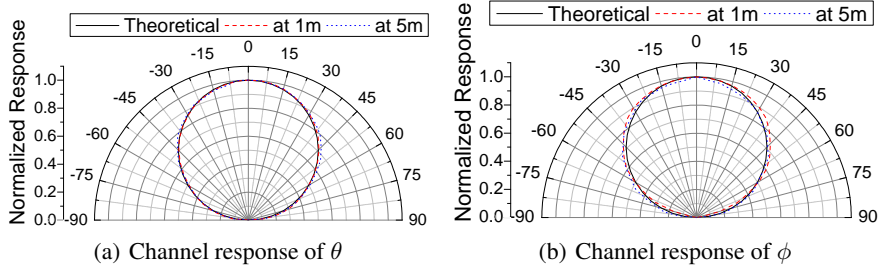


**Figure 3: Ideal and actual channel responses of the incidence angle  $\theta$  and irradiation angle  $\phi$  measured at 1m and 5m distances.**

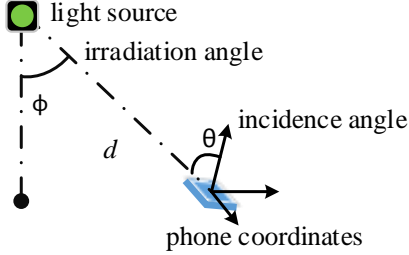


**Figure 2: The irradiation angle  $\phi$ , incidence angle  $\theta$ , and the distance between a light source and the receiver  $d$ .**

find a proper way to estimate the received energy under the constraints that LED's brightness may be *dimmed* via PWM.

## 2.2 Received Signal Strength

The light carrier from an LED is a pulse wave. Suppose the period of a 0-1 pulse wave is  $T$  with pulse time  $\tau$ . The Fourier series expansion for this pulse wave is

$$f(t) = \frac{\tau}{T} + \sum_{n=1}^{\infty} \frac{2}{n\pi} \sin\left(\frac{\pi n\tau}{T}\right) \cos\left(\frac{2\pi n}{T}t\right) \quad (3)$$

Above equation indicates that the emission power of the LED is *spread* over the baseband (the first AC component) and all the harmonics. Thus, it is nontrivial to measure the overall received energy. Fortunately, for sake of localization, we may measure some component energy as long as it validates the channel model in Eq. (2).

In particular, we measure *the energy that falls into the baseband*. Since a light sensor converts received energy into voltage, the actual received energy in the baseband is directly reflected in received signal strength, i.e., proportional to the coefficient of the first AC component in Eq. (3), i.e.,  $P_t \propto \frac{2}{\pi} \sin(\pi\tau/T)$ . Note that  $P_t$  is *not* affected by the actual baseband frequency. Thus we can measure the energy at any frequency, and thus suits our frequency hopping scheme (see §3) well. In addition,  $P_t$  is a function of duty cycle  $\tau/T$ , and symmetric around the duty cycle of 50% at which the maximum  $P_t$  is obtained. That is, we have  $P_t(\alpha) = P_t(1 - \alpha)$  where  $\alpha = \tau/T$  is the duty cycle of PWM. In consequence, the received signal strength  $P_r$  is now:

$$P_r = P_t(\alpha) \cdot H(d) \cdot G_r \quad (4)$$

This insight indicates that the light source also needs to convey the duty cycle information in its beacon for the receiver to correctly calculate the channel gain.

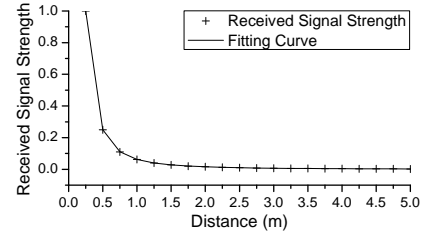


**Figure 4: RSS versus the distance  $d$ , both  $\theta$  and  $\phi$  are fixed to  $0^\circ$ .**

## 2.3 Channel Model for Localization

The accuracy of distance measurement is directly affected by our way of RSS measurement and the channel gain model. We determine the actual model and its parameters through real measurements.

**Incidence angle and irradiation angle:** We first examine the received energy versus the incidence angle  $\theta$  and the irradiation angle  $\phi$ . We measured the observed channel response for  $\theta \in [-90^\circ, 90^\circ]$  and  $\phi \in [-90^\circ, 90^\circ]$ , at distance 1m and 5m from the light source. The normalized measurement results are also plotted in Figure 3(a) and 3(b) in red dashed curve and blue dotted curves, respectively.

We also plot the cosine function of  $\theta$  and  $\phi$ , which is shown in black solid curve in Figure 3(a) and 3(b), respectively. From Fig. 3(a) and 3(b), we can see that the real measurements fit well with the cosines of  $\theta$  and  $\phi$ .

**LED-receiver distance:** According to Eq. (2), the received energy falls off as the square of the distance  $d$ . We verify this inverse square law by fixing the incidence and irradiation angles to  $0^\circ$  and vary the distance from 1m to 5m at 0.25m steps. The measured channel responses are shown with scatters in Figure 4. We fit the scatters with function  $C/d^2$  where  $C$  accounts for the constant coefficients in Eq. (2) and is fit to 0.0018. From Figure 4, we could see the overall fitting error is very small, with RMSE being  $1.85e-4$ . Therefore, the inverse square model accurately characterize the relation between the distance and the RSS.

**Channel Model for Localization:** With the insight gained above and the experimental verification, we conclude the channel model for our proposed RSS measurement method as follows:

$$P_r = C \cdot \sin(\alpha\pi) \cdot \frac{\cos\theta \cdot \cos\phi}{d^2} \quad (5)$$

where  $C$  is a constant that is jointly determined by the maximum power of the LED and the receiver gain of the light sensor, both can be calibrated once for all, and  $\alpha$  is the current duty cycle of the LED that is included in its beacon. It is essentially a zeroth-order model Lambertian model with additional adaptation to our way of RSS measurement. With this model, the distance can be precisely derived with the measured RSS, provided known  $C$ ,  $\theta$  and  $\phi$ .

## 3. BEACONING WITH VISIBLE LIGHT

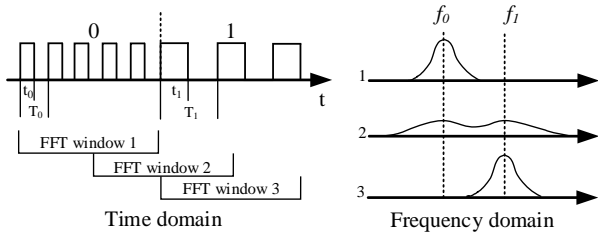


**Figure 5: Illustration of BFSK modulation of symbols ‘01’, with 50% PWM duty cycle. Left: temporal waveform; Right: frequency domain signal.**

The PWM-based dimming mechanism of LED enables communication with visible light. In this section, we present our design to achieve reliable location beaconing.

### 3.1 Communication with BFSK

Many modulation schemes were proposed in VLC field, such as OOK, VPPM, CSK etc. They all can be adopted to carry location beacons in the light carrier. However, they require either sophisticated decoding logic or special hardware, and also special mechanism to avoid flickering problem. In this work, we adopt the binary frequency shift keying (BFSK) for modulation for its simplicity and the natural prevention of flicker – as long as the duty cycle remains the same at different frequencies, there is no flicker provided the carrier frequencies are always over 200 Hz.

In BFSK, the sender adjusts carrier frequency to  $f_0$  and  $f_1$  for a certain duration (termed *symbol length*) to represent symbol 0 and 1, respectively. The receiver demodulates the incoming BFSK signal by transforming (FFT) the sensed light signals in a decoding window, whose length equals to the symbol length, to the frequency domain, and performing a binary decision on the major frequency component. The transform is carried in a sliding fashion: each time the window advances by a fraction of the symbol length. Note that the demodulation of all the channels is conducted simultaneously and in parallel.

Figure 5 illustrates the waveform for symbols ‘01’ after modulation and the corresponding demodulation process. The left figure shows the waveform, where the duty cycle is 50%, i.e.,  $t_0/T_0 = t_1/T_1 = 0.5$ . The right figure shows FFT results corresponding to the three temporal snapshots of the signal. In windows 1 and 3, one can see the energy mainly distributes around  $f_0$  and  $f_1$ . The corresponding decoded bits are thus 0 and 1, respectively. In window 2, the energy spreads across  $f_0$  to  $f_1$ , and the output might be 0 or 1 if the measured energy at  $f_0$  or  $f_1$  is larger than the other.

### 3.2 Channelization and Hopping

The major challenge for reliably beaconing is the potential collisions that may be caused by the co-existence of multiple, uncoordinated, and unsynchronized light sources. The actual deployment of light sources (e.g., usually attached to ceiling) and straight transmission of light make it difficult for the light sources to sense each other, hence difficult to

coordinate among light sources via carrier sensing. This is very different from radio communication cases. Time division multiple access is not feasible as they require synchronization or a carrier sensing mechanism among senders.

We choose to channelize the whole available spectrum into multiple disjoint and evenly spaced sub-carriers, and make two neighboring sub-carriers into one channel. The overall spectrum is bounded by the minimum frequency to prevent human perceivable flickering and the minimum of LED bulb’s On/Off speed and the response speed of the light sensor on the receiver.

We adopt random channel hopping to avoid persistent collision among light sources. Each light source randomly picks one channel, transmits a beacon for a certain period (called a *hopping period*), and then hops to another channel. Collisions may happen, but can be easily worked around by taking multiple observations of the same LED. The traffic load of each beacon is fixed. An optimal trade-off between channel bandwidth and channel number can be explored to minimize the collision probability.

## 4. THE LOCALIZATION ALGORITHM

For each light source, we can obtain one equation as Eq. (5) after RSS measurement, which represents one distance measurement. For the  $i$ -th light source at position  $\langle x_i, y_i, z_i \rangle$ , we have

$$P_r(i) = C_i \cdot \sin(\alpha_i \pi) \cdot \frac{\cos \theta_i \cdot \cos \phi_i}{d_i^2} \quad (6)$$

where  $d_i$  is the Euclidean distance between the receiver (at unknown position  $\langle x_0, y_0, z_0 \rangle$ ) and the  $i$ -th light source,  $P_r(i)$  is the measured RSS for the  $i$ -th light source and  $C_i$  is a constant. Assume all light sources facing downward, we also have  $\cos \phi_i = |z_0 - z_i|/d_i$ .

If the light sensor faces squarely upward toward the ceiling, we will have  $\theta_i = \phi_i$ . Therefore, only three unknowns, namely  $x_0, y_0, z_0$ , remain for each light source. In real usage, the receiver (hence the light sensor) may be in arbitrary attitude. This would make  $\theta_i \neq \phi_i$ , which complicates the problem. Intuitively, we can leverage the gravity sensor to estimate the device’s attitude and transform back to the canonical horizontal attitude.

When we observe three or more light sources, we will have an equation set and we may uniquely solve all unknowns via Newton’s Method. If more than three light sources are observed, we end up an overdetermined equation set and we solve them using least mean square (LMS) method. In fact, in such circumstances, a better option is to select better light sources instead of using all of them. In Pharos, we empirically select the light sources with highest RSSes. The intuition is that light sources with higher RSSes tend to be closer and with smaller incidence/irradiation angles.

## 5. THE PHAROS SYSTEM

Putting them together, the overall system architecture of Pharos consists of two parts: one part resides on the LED

bulb and the other on the receiving device with a light sensor, such as a mobile phone. The LED bulb includes a configuration module which enables Pharos provider to configure the location of the LED, and a modulation module for transmitting the location beacon. A channel hopping logic unit is also included in precaution of collisions when multiple light sources co-exist. Note that, current Pharos features are not fully supported on a commercial LED bulb. But we demonstrate that it takes slight extra cost to enable them (see the below prototype). Moreover, as this localization technique prevails, it may become a standard design. On the receiver side, it consists three functional modules. The demodulation module receives the beacons from light sources and extract the location of every received light source. During the process of demodulation, the received signal strength (RSS) is also measured. The localization module resolves the receiver’s position from the location of light sources and their respective RSS.

Unlike the existing indoor localization systems that commonly adopt a client/server architecture, which heavily relies on the network access and is thus limited to only networked areas and further depends on a centralized backend service, Pharos achieves plug-and-play effect. A user can simply replace their existing light bulb, no matter where it is, with Pharos-compatible LED bulb. The localization service for the area under that LED’s coverage is immediately enabled.

**Prototype implementation:** In our prototype, we build a small LED lamp using a commercial LED (Model: Cree T6) [9] with 10W marked power, as shown in Figure 6. We add a peripheral control circuitry to program the beacons. We hoped to directly use mobile phones as receivers as they come with a light sensor. However, the OS has significantly restricted the sampling rate (e.g. up to 100 Hz). Without access to its driver, we cannot leverage the existing sensor. Therefore, we design an external light sensor board (merely a light sensor and a small battery) and connect it to the phone through the microphone line of the audio jack. Note that, the use of audio jack limits the communication band to half of the audio chip’s sampling rate, i.e., 22.05 kHz. We chose the band from 10 kHz to 19 kHz in our implementation. We divide the band into 30 channels (300Hz each) and set the data rate to 120 bps per channel. Each beacon contains 82 bits, taking about 0.7s for one hopping. The overall waiting time is around 2.1s.

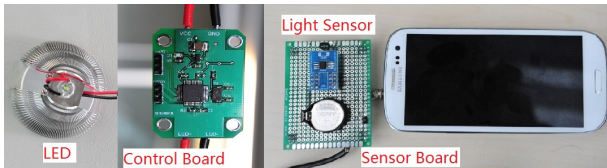


Figure 6: The hardware design of Pharos.

## 6. SYSTEM EVALUATION

**Experimental Settings:** We evaluated Pharos in two typical office environments: a conference room and a cubicle

area. We deployed 5 LED light sources for each environment. The environments and the deployed LEDs as shown in Figure 7. They represents different environmental complexity and have different reflection characteristics. The areas are 5m×8m, and 3.5m×6.5m, respectively. We place the phone at 60 positions on the floor, away from the user but with the presence of furniture, and run two test at each position. We offline trained and obtained the constant  $C_i$  for each LED.

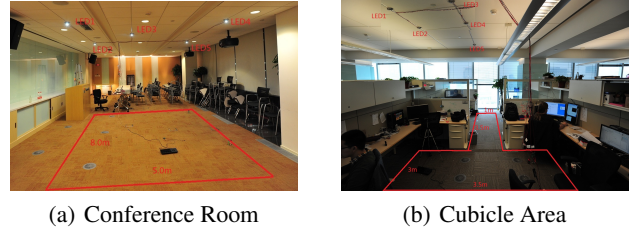


Figure 7: Deployments of Pharos in a conference room and a cubicle area, with five LEDs for each scenario.

**Methods for Comparison:** With visible LED light as location landmarks, we also compare with two intuitive algorithms in our experiments:

- Coverage Method: it locates a receiver to the position of the light source with the highest RSS.
- Weighted Average: it locates a receiver as the weighted average of the locations of the sensed light sources, using their RSS as weights.

**Localization Results:** Figure 8 plots the localization errors in two scenarios. It shows that Pharos yields high accuracy for both environments. The medium accuracy is around 0.3m and the 90 percentile accuracy is 0.45m and 0.7m for the conference room and the cubicle area, respectively. Compared with the conference room (almost empty), the cubicle environment is more complex with light reflection and shadowing and thus experience larger errors.

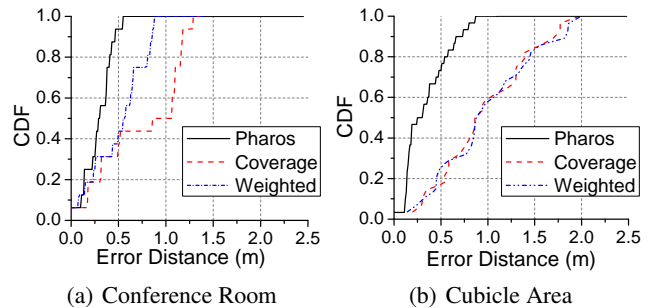


Figure 8: Localization accuracy in two environments.

We also examine the localization accuracy for each position in detail. We find that center area positions tends to have smaller errors than those outer positions. We omit the figure due to space limit. The reason is that center area positions have a better chance to reach light sources with smaller incidence angles. Moreover, the outside positions probably suffer from lighting reflection and shadowing.

Pharos always outperforms the Weighted Average method and pure Coverage method. By exploiting the characteristics of optical channels, Pharos improves the 90th accuracy by 1x (than Weighted Average) or 2x (than Coverage) in the conference room and about 1.5x (than both) in the cubical area. Similar gains are achieved for the average case.

**Comparison with WiFi-based Methods:** Current mainstream indoor localization systems are WiFi-based. We summarize the basic properties of representative WiFi localization systems, and compare them with Pharos. Their performances are excerpted from the original paper. We see that Pharos yields the best accuracy. Interesting, even with simple Coverage method, visible light based localization is already as good as the best WiFi localization system – Horus, which takes long time to construct a dense database. Note that, the latest development of WiFi-based localization may also achieve sub-meter accuracy, e.g., PinPoint [11] and ArrayTrack [20]. However, besides minor additional requirement on the infrastructure, they requirement multiple antennas and thus may be not applicable to a mobile phone.

Name	EZ [7]	Radar [4]	Horus [22]	Coverage	Pharos
Accuracy	2 - 7m	3 - 5m	~ 1m	~1m	~0.4m
Method	Model	FP	FP	FP	Model
Database	Yes	Yes	Yes	No	No
Overhead	Minimum	WD	WD	DC	DC

**Table 1: Comparisons with representative WiFi-based localization systems and coverage-based lighting localization. In the table, FP, WD and DC mean fingerprinting, war-driving and device configuration, respectively.**

## 7. ONGOING WORK

We have demonstrated that using visible light is a promising approach to high-accuracy localization. By exploiting the deployed lighting infrastructure, such a system provides a convenient positioning service for mobile users at almost-zero extra cost. However, this idea is still in its infancy. In this section, we briefly discuss ongoing work to address potential issues that may arise in real situations.

**Shadow and Reflection:** Similar to the multipath issue in WiFi-based localization, using visible light for localization may suffer from reflection or shadowing of lights. For example, when holding the phone in front of body, body reflection, especially in white shirt, will bring noises to localization. These issues are challenging but can be avoided or mitigated through carefully orienting the device, thanks to the visible nature of the light. We also plan to enhance signal processing in RSS measurement.

**LED Orientation:** We have assumed LEDs to be facing squarely down. In reality, this assumption may not always hold. We may need to make Pharos work with any LED orientation. To this end, we estimate the angle the LED from the downwards direction. One possible way to add a gravity sensor to the LED to directly measure the angle. An alternative way is to perform a calibration process.

**Device Diversity:** Different LEDs and light sensors may

have different emission power and receiving sensitivity, which would affect the distance measurement. Fortunately, as solid-state devices, these hardware-relevant properties are highly stable over the whole lifespan [1]. Thus, one time calibration is enough for each device. For practical use, we may reduce the calibration efforts, for example by automatically estimating the LED parameters as done for WiFi in [7].

**Insufficient Light Sources:** In some realistic situations, the number of available light sources may not be sufficient to automatically locate the user. For such situations, we may need to leverage other on-device sensors (e.g., IMU) and also involve the user for help by orienting the device to the light sources or performing certain simple gestures.

## 8. RELATED WORK

Most existing localization work leverages signals such as WiFi [7, 22, 4], FM [6], magnetism [8]. Our work is a radical deviation from these efforts. Here, we only review the closely related work, i.e., those dealing with visible lights.

**Visible Light based Indoor localization:** A few recent works also explore the idea of using visible light for localization [15, 17, 23, 21]. To our knowledge, Pharos is the first real working system whereas all existing studies are purely simulation work. In [21, 17], image sensors are used to locate the surrounding light sources based on the ray projection model. In [23] distances to multiple light sources are estimated by varying the transmitting power, which leads to unstable illumination. In [15], the authors infer TDOA from the peak-to-peak value of the interference signals from two LED lights. In contrast, in Pharos, we build accurate optical channel model applicable to localization with practical considerations like dimming and flickering avoidance, and working with multiple light sources.

**Visible Light Communication:** VLC aims to leverage visible lights as communication carriers. The recent standard IEEE 802.15.7 specifies the hardware, modulation, channel coding, and the MAC protocol for various applications [18]. A number of studies discuss optical channels for VLC such as [12, 10, 14]. While VLC research mainly focus on wide-band high-speed communication, we aim at low system complexity and robust broadcast for localization purpose.

## 9. CONCLUSION

In this paper, we present the design, implementation and evaluation of Pharos, a visible light based localization system that exploit LED lamps. The system has no dependency on network access and can be used immediately after proper configuring the LED bulb. We identified and tackled key technical challenges for reliable location beaconing, accurate distance estimation between LED bulbs and the receiver. We conducted preliminary evaluation in typical office environments and achieved sub-meter accuracy. Our work (so far) confirms the potential of visible light based localization as the key enabler towards fine grained physical analytics.

## 10. REFERENCES

- [1] Light Emitting Diode: Wikipedia.  
[http://en.wikipedia.org/wiki/Light-emitting\\_diode](http://en.wikipedia.org/wiki/Light-emitting_diode).
- [2] Physical analytics.  
<http://researcher.watson.ibm.com>.
- [3] Phytics: Physical analytics.  
<http://research.microsoft.com/en-us/projects/phytics/default.aspx>.
- [4] P. Bahl and V. N. Padmanabhan. RADAR: An In-Building RF-Based User Location and Tracking System. In *IEEE INFOCOM*, 2000.
- [5] J. R. Barry. *Wireless infrared communications*. Springer, 1994.
- [6] Y. Chen, D. Lymberopoulos, J. Liu, and B. Priyantha. FM-based indoor localization. In *ACM MobiSys*, 2012.
- [7] K. Chintalapudi, A. P. Iyer, and V. N. Padmanabhan. Indoor localization without the pain. In *ACM MOBICOM*, 2010.
- [8] J. Chung, M. Donahoe, and et al. Indoor location sensing using geo-magnetism. In *ACM MobiSys*, 2011.
- [9] CREE. <http://www.cree.com/>.
- [10] D. Giustiniano, N. O. Tippenhauer, and S. Mangold. Low-complexity visible light networking with led-to-led communication. In *Wireless Days (WD), 2012 IFIP*, pages 1–8. IEEE, 2012.
- [11] K. Joshi, S. Hong, and S. Katti. Pinpoint: localizing interfering radios. In *NSDI'13*.
- [12] T. Komine and M. Nakagawa. Fundamental analysis for visible-light communication system using led lights. *Consumer Electronics, IEEE Transactions on*, 50(1):100–107, 2004.
- [13] Nomi. <http://www.getnomi.com>.
- [14] D. C. O'Brien, L. Zeng, H. Le-Minh, G. Faulkner, J. W. Walewski, and S. Randel. Visible light communications: Challenges and possibilities. In *PIMRC 2008*, pages 1–5. IEEE, 2008.
- [15] K. Panta and J. Armstrong. Indoor localisation using white leds. *Electronics letters*, 48(4):228–230, 2012.
- [16] Business Insider.  
<http://www.businessinsider.com/retailers-track-customers-2013-7>.
- [17] M. Rahman, M. Haque, and K.-D. Kim. High precision indoor positioning using lighting led and image sensor. In *ICCIT*, 2011.
- [18] S. Rajagopal, R. D. Roberts, and S.-K. Lim. Ieee 802.15. 7 visible light communication: modulation schemes and dimming support. *Communications Magazine, IEEE*, 50(3):72–82, 2012.
- [19] Walkbase. <http://www.walkbase.com>.
- [20] J. Xiong and K. Jamieson. Arraytrack: a fine-grained indoor location system. In *NSDI'13*.
- [21] M. Yoshino, S. Haruyama, and M. Nakagawa. High-accuracy positioning system using visible led lights and image sensor. In *Radio and Wireless Symposium*, 2008.
- [22] M. Youssef and A. K. Agrawala. The Horus WLAN location determination system. In *ACM MobiSys*, 2005.
- [23] W. Zhang and M. Kavehrad. A 2-d indoor localization system based on visible light led. In *Photonics Society Summer Topical Meeting Series*, 2012.